

Large-scale Computation of the Pump-Turbine Rotating Stall

Olivier PACOT* , François AVELLAN* and Chisachi KATO**

1. Introduction

Pump-turbines are nowadays getting more popular in hydropower plant, as it reduces construction and maintenance costs. However, such machines are often operated at off-design condition resulting in a loss of efficiency. A known phenomenon resulting from the off-design operation in pumping mode is the rotating stall. The rotating stall is a phenomenon recognizable by the presence of rotating cells in the diffuser. Such cells could be stationary, forward or backward rotating with regard to the impeller rotation direction. Although, such phenomenon was discovered more than half a century ago¹⁾, it has not yet been fully understood. The reason is that experimental and numerical investigations are not trivial, as the phenomenon occurs in a complex three dimensional geometry involving rotating and stationary components. Experimentally, the main drawback is the difficulties to get optical access into the machine under operation. It requires to manufacture specific components equipped with Plexiglas windows to investigate only small area of the flow. Numerically, the main drawback is the ability to compute complex flows using standard computing resources accurately. Simplified approaches, as the Reynolds Averaged Navier-Stokes (RANS) method, were used in order to reduce the computing resources requirement considerably. However, past studies have shown the limitation of such approaches to compute accurately the rotating stall phenomenon²⁾.

Based on the recent opportunity to access supercomputer like K³⁾, the present research focuses on the possibility to investigate the rotating stall phenomena using the Large Eddy Simulation (LES) method. Such method is more time and resources demanding, but is more promising for computing complex flows accurately. However, to ensure that such computation is realistic, a feasibility study has to be performed in order to evaluate the resource requirements such as the mesh size and the computing resources.

The feasibility study of the present computation is introduced

in section 2. Then, sections 3 and 4 describe the governing equations and the numerical method, respectively. Finally, results of the flow initialization are shown in section 5 with the concluding remarks in section 6.

2. Feasibility Study

To accurately simulate turbulent flows, all the important structures present in the flows should be computed. The spatial resolution should thus be fine enough to capture the smallest important scales and the computational region should be large enough to allow the largest scales to behave unaffectedly by the region. Based on the ratio between the largest and the smallest length scales, one can estimate the number of elements to capture all eddies⁴⁾. Such ratio is proportional to $Re^{3/4}$, leading to a mesh size requirement proportional to $Re^{9/4}$. Re is the Reynolds number and is defined as follow: $Re=UL/\nu$, where U and L are respectively the characteristic velocity and length and ν being the kinematic viscosity of the fluid. Nevertheless, even with the use of the latest supercomputers, such requirement is still not affordable for industrial applications. That is why the Large Eddy Simulation method was selected to compute the rotating stall. This method is less constraining, because only the non-filtered structures are explicitly computed. However, estimation on the mesh size, regarding the needs of the computation, remains necessary.

2.1. Mesh Requirement

In the present study, the interest focuses on the wall bounded turbulent flow present in the diffuser of the pump-turbine. As the flow is bounded by the wall it implies the resolution of turbulent boundary layers and as the flow is near the outlet of the impeller it implies a high velocity magnitude. In what follows, the reference length, L , is the chord length of the diffuser guide vane and the reference velocity, C , is the absolute velocity obtained from the velocity triangles at the impeller outlet.

To accurately simulate a turbulent boundary layer, one has to compute the coherent structures, which are streamwise vortices near wall. These coherent structures are located inside the buffer layer ($y^+ \approx 5-30$)⁵⁾, thus imposing a fine discretization of

*Laboratory for Hydraulic Machines, EPFL, Switzerland

**Institute of Industrial Science, The University of Tokyo, Japan

研 究 速 報

the flow near walls^{6),7)}. The typical dimensions of these coherent vortical structures are given in Table 1 in term of wall unit, defined as: $\Delta^+ = \Delta u_\tau / \nu$, where u_τ is the friction velocity.

Table 1 Dimensional and non-dimensional streamwise vortices size, for a Reynolds number of 1.9 million.

	<i>Vortex diameter</i>	<i>Vortex length</i>	<i>Vortex spacing</i>
Δ^+	30	300	150
Δ [mm]	0.037	0.37	0.19

In order to estimate the expected size of those vortices, the viscous length $l^+ = \nu / u_\tau$ has to be determined, which consists in determining the friction velocity. This is achieved using the following formulas^{7), 8)} relating the mean flow velocity to the friction velocity using the wall skin friction coefficient c_f :

$$\frac{u_\tau}{C} = \sqrt{\frac{c_f}{2}}$$

$$c_f = 0.0577 \text{Re}_x^{-1/5} \text{ for } \text{Re}_x \leq 10^6$$

$$c_f = 0.027 \text{Re}_x^{-1/7} \text{ for } 10^6 \leq \text{Re}_x \leq 10^9$$

For a Reynolds number of 1.9 million, the ratio between the friction velocity and the absolute velocity is 4% giving a viscous length of 1.24 μm . The expected dimensions in mm of these streamwise vortices are also given in Table 1.

To estimate the total number of elements, it is assumed that the flow passage between two diffuser guide vanes can be represented by a rectangular box with the following dimension: 100 x 75 x 35 mm representing the streamwise, transverse and spanwise directions respectively. Furthermore, to estimate the total number of elements for the full pump-turbine, it is assumed that the pump-turbine has 87 such flow passages. Finally, to compute the number of elements per direction, the following spatial discretization was selected: $\Delta x^+ = 50$, $\Delta y^+ = \Delta z^+ = 20$. This estimation has resulted in that the present computation will need 600 billion of elements. This is of course not feasible and the following change was adopted: based on the Reynolds-number similarity, the Reynolds number was reduced by a factor 5 in order to reach a realistic spatial discretization. The new required mesh is about 8 billion, which is nowadays affordable.

2.2. Computing Resources Requirement

Since estimation on the mesh size is carried out, one can estimate the computing resources in term of memory size, amount of computing nodes and resources use duration requirement.

To perform this estimation, some characteristics of the CFD software and the computation are necessary. In the present

research, computation will be performed using the in-house Front Flow Blue (FFB) software. This software has been already successfully ported to several supercomputer architectures and time measurements have shown that the sustained peak performance of the code is about 5% of the peak performance, FFB requires about 20k FLOP per element per time step and that the appropriated load balancing is 0.1 million elements per a processor core.

As introduced previously, the estimated size of the mesh is 8 billion elements. Furthermore, the time discretization is 10,000 time steps per impeller revolution and the number of impeller revolutions to compute to perform statistics is 40.

The computation will be performed on the supercomputer K, belonging to RIKEN. This supercomputer features 8 cores per compute nodes, a total number of compute nodes over 80,000 for a peak performance of 128 GFLOPS per compute node.

Using the above information, the computation requires 10,000 compute nodes and one impeller revolution last 7 hours. This results in the computation of 40 impeller revolutions for 12 days.

The feasibility study showed thus that such computation is nowadays possible and that thanks to important resources, results can be obtained in a reasonable time.

3. Governing Equations

The governing equations to compute incompressible flows by the LES method are the continuity equation and the incompressible low-pass filtered Navier-Stokes equations:

$$\frac{\partial \bar{u}_i}{\partial x_i} = 0$$

$$\frac{\partial \bar{u}_i}{\partial t} + \bar{u}_j \frac{\partial \bar{u}_i}{\partial x_j} = -\frac{1}{\rho} \frac{\partial \bar{p}}{\partial x_i} + \frac{\partial}{\partial x_j} \left[\nu \left(\frac{\partial \bar{u}_i}{\partial x_j} + \frac{\partial \bar{u}_j}{\partial x_i} \right) - \tau_{ij} \right]$$

where \bar{u}_i is the filtered velocity component, \bar{p} is the filtered static pressure, ρ is the fluid density, ν is the fluid kinematic viscosity and τ_{ij} is the subgrid scale tensor (SGS), defined as:

$$\tau_{ij} = \overline{u_i u_j} - \bar{u}_i \bar{u}_j$$

To close the system of equations, the Smagorinsky model⁹⁾ defined as follow is used:

$$\tau_{ij} - \frac{1}{3} \delta_{ij} \tau_{kk} = -2 \nu_{SGS} \bar{S}_{ij}$$

with

$$\nu_{SGS} = (C_s \Delta)^2 \sqrt{2 \bar{S}_{ij} \bar{S}_{ij}} \text{ and } \bar{S}_{ij} = \frac{1}{2} \left(\frac{\partial \bar{u}_i}{\partial x_j} + \frac{\partial \bar{u}_j}{\partial x_i} \right)$$

where C_s is the Smagorinsky constant and Δ is the size of the grid filter. In the present code, the Smagorinsky constant is

evaluated locally using the model proposed by Lilly¹⁰⁾ which is a modified model of the Dynamic Smagorinsky Model introduced by Germano¹¹⁾.

4. Numerical Method

The filtered incompressible Navier-Stokes equations are solved using the Fractional Step (FS) method with the Crank-Nicolson (CN) implicit time integration scheme. The spatial discretization is performed by the Galerkin Finite Element Method. The resulting linear systems of equations are solved by the Bi-CGSTAB¹³⁾ wrapped with the residual cutting method (RCM).¹⁴⁾ The numerical code has a multiple frame of references implemented and uses an overset grid¹²⁾ as interface.

5. Results

Figure 1 shows the flow velocity magnitude in the impeller and in the diffuser at the mid-plane height. This flow is obtained after computing 23 impeller revolutions with an initial zero velocity flow field. The mesh used to initiate the flow is a coarse mesh composed of 85 million elements and computations were performed using a supercomputer FX-10, belonging to the University of Tokyo. FX-10 possesses the same architecture as K except that it has 16 cores per compute node. The pump-turbine is operating in pumping mode and at a part load condition, $Q/Q_{BEP}=76\%$, with the corresponding part load flow coefficient $\phi=0.026$; BEP standing for best efficiency point.

As it can be seen on Figure 1, the flow rate through the diffuser passages is not regular. Mainly, four diffuser passages experience a high flow rates whereas the flow in the neighboring passages seem to be blocked. As the purpose of this computation is to simulate the rotating stall, such result is encouraging since it corroborates the experimental results of Braun²⁾, who reported the presence of four rotating cells in such operating condition.

At this stage of the initialization process, one can notice that the flow is already developed in the impeller whereas the flow in the spiral casing, outer part of the diffuser, seems still at rest. The reason for this is that the volume of fluid in the spiral casing is 15 times greater than the volume of fluid inside the impeller, resulting in the observed lower flow velocity magnitude.

Figure 2 shows the flow velocity magnitude in the impeller and in the diffuser at the same location as in Figure 1, for the flow obtained after the computation of 33 impeller revolutions. As it can be seen, there is still four diffuser passages experiencing a high flow rate, but appearing in approximately 2-2.5 diffuser passages further in the same direction as the

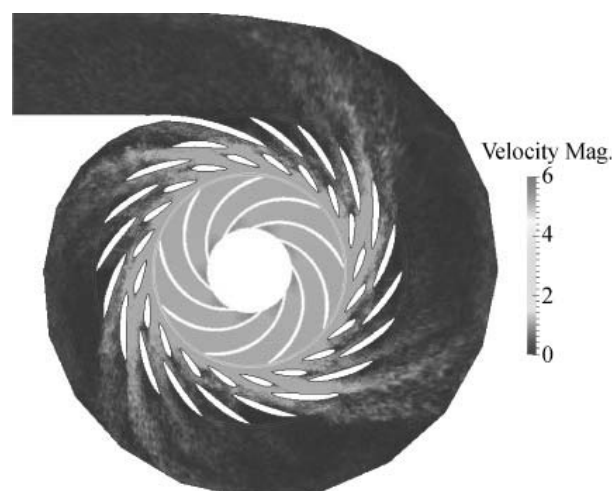


Figure 1 Instantaneous flow velocity magnitude in the mid plane of the pump-turbine after 23 impeller revolutions computation.

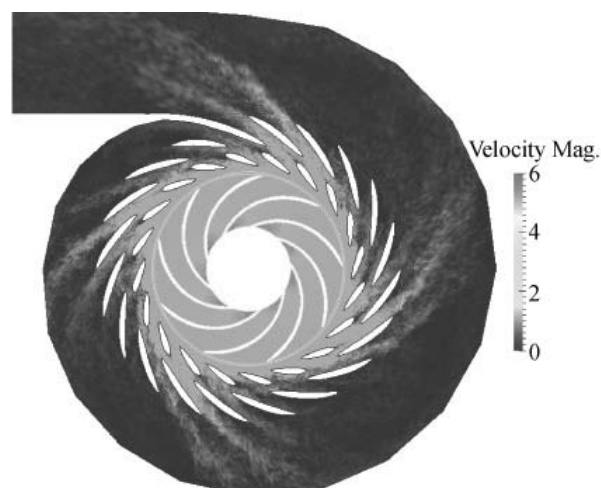


Figure 2 Instantaneous flow velocity magnitude in the mid plane of the pump-turbine after 33 impeller revolutions computation.

impeller revolution. This shifting gives, as a rough approximation, a propagation speed of 1 diffuser passage for 4 impeller revolutions which is about twice slower than what Braun reported²⁾.

Figure 3 shows the instantaneous streamlines, after 33 impeller revolutions, passing through the guide vane throat (T). As it can be seen, the flow inside the diffuser is well destabilized and does not follow the direction imposed by the diffuser geometry. In the diffuser passages (1) and (2), we can clearly see that the flow is highly deviated. Instead of exiting through their respective diffuser passage, some portion of the flow deviates and goes into the neighboring passage.

In the diffuser passage (3), the streamlines show that the flow

is going to the pressure side of the guide vane, where some streamlines go to the leading edge of the guide vane whereas others go to the trailing edge. This demonstrates that the diffuser channel (3) is experiencing some reverse flow, thus

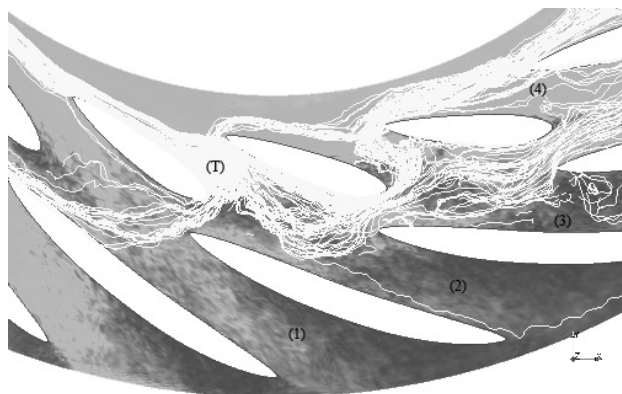


Figure 3 Instantaneous streamlines, after 33 impeller revolutions, passing through the guide vanes throat (T).

explaining why some passages have a higher flow rate than others. The same observation can be done for the diffuser passage (2). In the zone (T), some streamlines are going backward (reverse flow), whereas others are going forward. This streamline superimposition shows that the physics taking place in that area is fully 3D. Furthermore, one can notice that once the streamlines pass the trailing edge of the guide vane, such streamlines do not go through the neighboring passage (4) but go to the next one. This confirms that the flow between the impeller and the guide vanes is highly circumferential, which is expected when operating the pump-turbine at a part-load condition.

Furthermore, referring to Figure 3, one can notice that the stall pattern in the present computation occupies two diffuser passages whereas the experiment reported only one diffuser passage. Such difference can be explained, as previously mentioned, by the high circumferential flow velocity. As reported by Sinha¹⁵⁾, an increase of the circumferential velocity results in stall-cell size extension from one to two diffuser passages which can explain the lower propagation speed computed presently.

6. Conclusion

The purpose of the present study is to simulate the rotating stall phenomenon appearing in a pump-turbine operating in pumping mode at a part load condition, $Q/Q_{BEP}=76\%$, using the LES method. To ensure that such a computation is affordable, a

feasibility study was performed. As the phenomenon occurs in a complex geometry, involving the resolution of turbulent boundary layers, it was shown that, still today, even with the fast development of the computing resources, such computation is not affordable as it requires a mesh composed of 600 billion elements. Therefore, the Reynolds number was reduced by a factor 5 resulting in a mesh requirement of 8 billion elements. Furthermore, thanks to the access to large supercomputer as K, it was shown that results could be obtained in a reasonable time.

The flow field was initialized using a coarse mesh, composed of 85 million elements and setting the initial flow field to a zero velocity field. It was shown that after several impeller revolution computations, the expected instability took place and this even with the use of the coarse mesh. However, the computed rotating stall propagation speed is about twice smaller than the experimental one. One possible reason is in a higher circumferential flow velocity computed resulting in a stall-cell size of two diffuser passages and in a lower stall propagation speed.

Acknowledgment

The author would like to thank Dr. Y. Guo and Mr. Y. Yamade for all their scientific advices and for providing the numerical code. This research was supported by the Swiss National Science Foundation (SNSF) Grant No. 130605.

(Manuscript received. January 4, 2013)

References

- 1) Emmons, H.W., et al., *ASME J. Basic Eng.*, 81, (1959), pp409-416.
- 2) Braun, O., *PhD thesis*, EPFL (2009).
- 3) Miyazaki, H., et al., *FUJITSU Sci. Tech. J.*, 48, (2012), pp255-265.
- 4) Piomelli, U. and E. Balaras, *Ann. Rev. Fluid Mech.*, 34, (2002), pp349 - 374.
- 5) Robinson, S.K., *Annu. Re. Fluid Mech.* 23, (1991), pp 601-639.
- 6) Chapman, D., *AIAA journal*, 17, (1979), pp1293-1313
- 7) Choi, H, and P. Moin. *Phys. Fluids*, 24, 1(2012), pp011702-011702-5.
- 8) Schlichting, H., *McGraw-Hill*, New York (1955).
- 9) Smagorinsky, J., *Mon. Weather Rev.*, 91, 3(1963), pp99-164.
- 10) Lilly, D.K., *Phys. Fluids. A*, 4, 7(1992), pp633-635.
- 11) Germano, M., et al., *Phys. Fluids. A*, 3, 7(1991), pp1760-1765.
- 12) Kato, C., et al., *Trans. ASME J Applied Mech.*, 70, (2003), pp32-43.
- 13) Van de Vorst, HA., *SIAM J Sci Statist. Comput.*, 13, 2(2002), pp631-644.
- 14) Tamura, A., et al., *J Computat. Phys.*, 137, (1997), pp247-264.
- 15) Sinha, M., Pinarbasi, A. and Katz, J., *Trans ASME, J. Fluids Engn*, 123, (2001), pp490-499.